

that intrinsically available in the multiphoton absorption process.

Significant increases in the overall efficiency of an isotopic segregation scheme may be achieved by irradiation of a low-pressure mixture of reactant in an excess of effective coreagent and by cooling the sample and reaction vessel. However, a greater increase in selectivity and end product enrichment could be realized by a more judicious choice of IR laser frequency or frequencies. Our technique allows us to rapidly assay relative isotopic dissociation probabilities and choose appropriate wavelengths to provide both high selectivity and high yields. Our studies only require microscopic quantities of isotopically enriched reagent (i.e., a few micrograms). In a system analogous to those of Ritter and Freund one should observe macroscopic isotopic segregations consistent with an average selectivity of $\alpha > 100$ for the dissociation of $^{12}\text{CF}_2\text{Cl}_2$ at $10.7 \mu\text{m}$ (the P(30) line at 934 cm^{-1}) and of $1/\alpha \approx 30$ for carbon-13 enriched product species at $9.5 \mu\text{m}$ (the P(8) line at 1057 cm^{-1}). These represent substantial increases over the values of 5 and 1.04 reported previously.

Very few attempts have been successful in the selective segregation of rare isotopes into product species using IR multiphoton dissociation techniques. As demonstrated by the work of Ritter and Freund, the low carbon-13 dissociation selectivities result in negligible product array enrichments; it is then preferable to dissociate $>90\%$ of the sample with selectivity for carbon-12 decomposition.

By using real-time LEF diagnostics to determine collision-free dissociation probabilities for each isotopic species, one can very rapidly assess optimum IR wavelengths for the selective multiphoton dissociation of rare isotopic species. This allows one to design experiments to selectively perturb those isotopic species of lesser abundance. Provided it is possible to scavenge the initially formed intermediates without encouraging secondary photolysis, scrambling, or nonselective thermal processes, one may realize a maximum isotopic enrichment of $^{13}\beta_{\text{P,max}} = R_{\text{P}}/R_0 = 1/\alpha_0$ for the products.

Acknowledgment. We gratefully thank Dr. Joseph J. Ritter for providing us with the isotopically enriched and synthetically purified samples of $^{13}\text{CF}_2\text{Cl}_2$ and the valuable assistance of Drs. J. J. Ritter, Richard E. Rebbert, and Marilyn Jacox in materials purification and analysis. This work received partial support from the Department of Energy under Contract No. EA-77-A-01-6010, task No. A-058.

References and Notes

- (1) R. V. Ambartsumyan and V. S. Letokhov, *Acc. Chem. Res.*, **10**, 61 (1977); V. S. Letokhov and C. B. Moore, *Sov. J. Quantum Electron. (Engl. Transl.)*, **6**, 129 (1976); C. D. Cantrell, S. M. Freund, and J. L. Lyman, "Laser Handbook", Vol. 3, M. Stitch, Ed., North-Holland Publishing Co. (to be published), and references therein.
- (2) In keeping with the notation of Lyman and Rockwood,³ we shall define the enrichment factor, β_r , for the reactant species as $\beta_r = R_r/R_0$, where R_0 is the normal isotope ratio and R_r is the isotope ratio of the reactant remaining after irradiation. Likewise, the enrichment factor for the product species is given as $\beta_p = R_p/R_0$, where R_p is now the isotope ratio of the products. We also define the selectivity factor, α , by $dn_1/dn_2 = \alpha n_1/n_2$, where n_1 and n_2 are the concentrations of two isotopic species.
- (3) J. L. Lyman and S. D. Rockwood, *J. Appl. Phys.*, **47**, 595 (1976).
- (4) (a) J. J. Ritter and S. M. Freund, *J. Chem. Soc., Chem. Commun.*, 811 (1976); (b) J. J. Ritter, *J. Am. Chem. Soc.*, **100**, 2441 (1978).
- (5) Certain commercial materials and equipment are identified in this paper in order to specify adequately the experimental procedure. In no case does such identification imply recommendation or endorsement by the National Bureau of Standards, nor does it necessarily imply that the material or equipment identified is necessarily the best available for the purpose.
- (6) D. S. King and J. C. Stephenson, *Chem. Phys. Lett.*, **51**, 48 (1977); J. C. Stephenson and D. S. King, *J. Chem. Phys.*, **69**, 1485 (1978).
- (7) J. Morcillo, L. J. Zamorano, and J. M. V. Heredia, *Spectrochim. Acta*, **22**, 1969 (1966); E. K. Plyer and W. S. Benedict, *J. Res. Natl. Bur. Stand.*, **47**, 202 (1951).
- (8) C. S. Parmenter and M. W. Schuyler, *Chem. Phys. Lett.*, **6**, 339 (1970).
- (9) D. S. King, P. K. Schenck, and J. C. Stephenson, "Spectroscopy and Photophysics of the $\text{CF}_2 \text{ A}^1\text{B}_1 - \text{X}^1\text{A}_1$ System" (in process of publication).
- (10) G. Folcher and W. Braun, *J. Photochem.*, **8**, 341 (1978).
- (11) J. W. Hudgens, *J. Chem. Phys.*, **68**, 777 (1978).
- (12) Aa. S. Sudbo, P. A. Schulz, E. R. Grant, Y. R. Shen, and Y. T. Lee, *J. Chem. Phys.*, **68**, 1306 (1978).
- (13) D. E. Milligan, M. E. Jacox, J. H. McAuley, and C. E. Smith, *J. Mol. Spectrosc.*, **45**, 377 (1973).
- (14) S. Bittenson and P. L. Houston, *J. Chem. Phys.*, **67**, 4819 (1977).

Carbon-13 Magnetic Shielding from Beam-Maser Measurements of Spin-Rotation Interaction in Acetonitrile

S. G. Kukolich,*^{1a} G. Lind,^{1a} M. Barfield,^{1a} L. Faehl,^{1b} and J. L. Marshall^{1b}

Contribution from the Departments of Chemistry, University of Arizona, Tucson, Arizona 85719, and North Texas State University, Denton, Texas 76203. Received May 1, 1978

Abstract: The $J = 1 \rightarrow 0$ transitions in $\text{CH}_3^{13}\text{CN}$ were observed using a beam maser spectrometer at 6-kHz line width (fwhm) and a ^{13}C -enriched sample. The strongest component was observed with natural-abundance $\text{CH}_3^{13}\text{CN}$. Spectra of $\text{CH}_3^{12}\text{CN}$ were obtained at higher resolution using Ramsey's method of separated oscillating fields. For $\text{CH}_3^{12}\text{CN}$ we obtain $eqQ_{\text{N}} = -4224.4 \pm 0.7 \text{ kHz}$, $C_{\text{N}} = 2.0 \pm 0.4 \text{ kHz}$, $C_{\text{H}} = -0.6 \pm 0.4 \text{ kHz}$, and a $J = 1 \rightarrow 0$ transition center frequency of $18\,397\,783.5 \pm 0.7 \text{ kHz}$. For $\text{CH}_3^{13}\text{CN}$ the $J = 1 \rightarrow 0$ transition center frequency is $18\,388\,681.0 \pm 2.0 \text{ kHz}$ and we obtain $eqQ_{\text{N}} = -4224.6 \pm 1 \text{ kHz}$ and $C_{\text{N}} = 1.9 \pm 0.5 \text{ kHz}$. The ^{13}C spin-rotation strength in $\text{CH}_3^{13}\text{CN}$ was determined in this study to be $3.6 \pm 0.2 \text{ kHz}$ and this leads to a value of $\sigma_{\perp} = -11 \pm 14 \text{ ppm}$.

I. Introduction

Rotational transitions and nitrogen quadrupole coupling in CH_3CN were first reported² in 1950. It is a favorable molecule for microwave study because of its large dipole moment ($\sim 4 \text{ D}$). More recently, Lamb-dip spectra in the microwave

region were obtained by Costain.³ Beam-maser transitions in CH_3CN and CD_3CN were observed in our earlier work,⁴ and D quadrupole and ^{14}N quadrupole coupling strengths were reported.

The relationship between spin-rotation tensor elements and magnetic shielding tensor elements has been discussed by

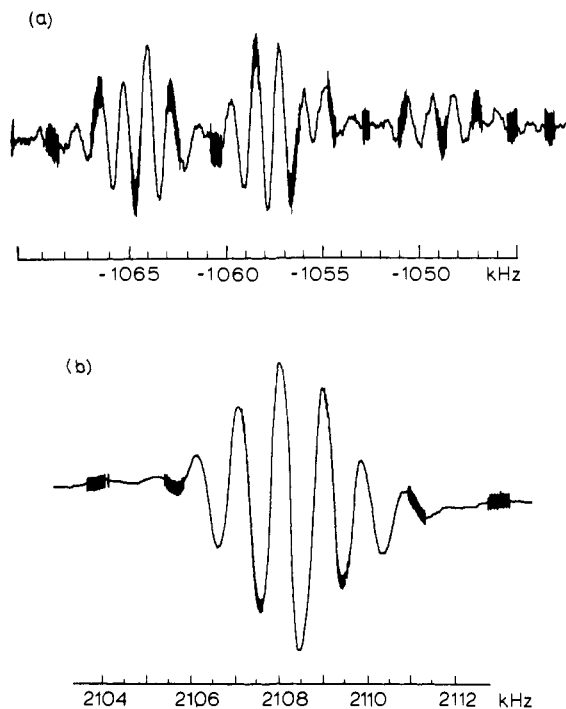


Figure 1. Recorder tracings of experimental spectra of $F_{1'} = 1$ (a) and $F_{1'} = 0$ (b) components of $J = 1 \rightarrow 0$ transitions in $\text{CH}_3^{12}\text{CN}$. Frequencies are in kilohertz relative to the line center at 18 397 783.5 kHz.

Ramsey⁵ and by Flygare.⁶ This relationship was recently used to determine proton magnetic shielding tensors for H_2CO and NH_3 .⁷ Values of ^{13}C magnetic shielding components from molecular-beam studies of ^{13}CO ⁸ and O^{13}CS ⁹ have been used¹⁰ in conjunction with theoretical values to establish an absolute ^{13}C chemical shielding scale. In the present study, the relationship between spin-rotation constants and magnetic shielding constants for $\text{CH}_3^{13}\text{CN}$ was of particular interest because of the apparent disagreements in the chemical shielding anisotropy and isotropic chemical shifts for studies carried out in the nematic liquid crystal and in the solid phases. Polarization transfer results for solid $\text{CH}_3^{13}\text{CN}$ gave a value of $\sigma_{\parallel} - \sigma_{\perp} = 204$ ppm¹¹ and $\sigma_{\text{av}} = 47$ ppm (relative to $^{13}\text{CS}_2$)¹² for the ^{13}C of the nitrile. Independent studies^{12,13} of $\text{CH}_3^{13}\text{CN}$ partially oriented in the nematic liquid crystal phase gave anisotropies of 302¹² and 307 ppm¹³ but isotropic shielding values are close to the standard liquid-phase value of 76 ppm (relative to $^{13}\text{CS}_2$)^{10,12}. It was generally believed that such large disparities could not be due to medium effects alone and that the gas-phase results would be in better conformity with one or other of the two sets of data.

In the present work the ^{13}C spin-rotation interaction strength is obtained from molecular-beam measurements. The "gas-phase" value for the spin-rotation constant is used to obtain the paramagnetic contribution to the magnetic shielding tensor. Combining this result with recent, accurate semiempirical values for the diamagnetic contribution to the shielding gives the total value. This value is compared with the solid-phase and liquid-crystal-phase results as well as with the theoretically determined value.

II. Experimental Section

The spectra for the $J = 1 \rightarrow 0$ transitions in $\text{CH}_3^{12}\text{CN}$ and $\text{CH}_3^{13}\text{CN}$ were recorded using a molecular beam maser spectrometer. The spectrometer was described earlier.¹⁵ The basic design is similar to the original maser.¹⁶ For the present measurements a 0.1-mm heated-nozzle source was used. The best spectra were obtained with the nozzle temperature at 60 °C and the sample at 55 °C.

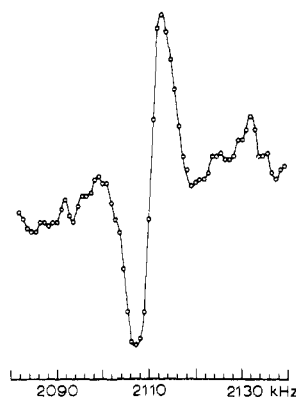


Figure 2. Computer-averaged experimental spectrum for the $F_{1'} = 0$ component of the $J = 1 \rightarrow 0$ transition in $\text{CH}_3^{13}\text{CN}$. This spectrum was obtained for ^{13}C in natural abundance in a sample of acetonitrile. The open circles are experimental points and these are connected by the solid line.

The $\text{CH}_3^{12}\text{CN}$ spectra were recorded using a two-cavity system¹⁵ to obtain Ramsey-type spectra with better resolution. The width of the central resonance was about 0.4 kHz. The two-cavity spectra are somewhat weaker than single-cavity spectra, but this is not a problem with $\text{CH}_3^{12}\text{CN}$ since we can use 10–15 g in a single run. The $J = 1 \rightarrow 0$ rotational spectrum of $\text{CH}_3^{12}\text{CN}$ consists of three groups of lines with $F_{1'} = 0, 1$, and 2. The angular momentum operator $\mathbf{F}_1 = \mathbf{I}_N + \mathbf{J}$, where \mathbf{I}_N and \mathbf{J} denote the nitrogen nuclear spin operator and rotational angular momentum operator, respectively, and $F_{1'}$ refers to the $J = 1$ state. A typical spectrum for the $F_{1'} = 1$ and $F_{1'} = 0$ components is shown in Figure 1.

The $\text{CH}_3^{13}\text{CN}$ spectra were recorded using the more conventional single-cavity system giving the Rabi-type resonance. Cavities of 18- and 25-cm lengths were used, and the observed line width was 5.5 kHz (fwhm). The $F_{1'} = 0$ component of the $J = 1 \rightarrow 0$ transition for $\text{CH}_3^{13}\text{CN}$ could be observed using the natural abundance of ^{13}C in the CH_3CN sample. Ten spectra were recorded on a digital tape recorder and the averaged spectrum is shown in Figure 2.

The $F_{1'} = 1$ and $F_{1'} = 2$ components are weaker than the $F_{1'} = 0$ component, and ^{13}C -enriched samples were used to obtain data more quickly and efficiently. The sample of acetonitrile- ^{13}C was prepared by the following procedure: a thick-walled test tube was charged with 1.5 g of potassium cyanide- ^{13}C (>90% isotopic enrichment; purchased from Koch Isotopes, Cambridge, Mass.), washed in with 3 mL of water, and 4.9 g of freshly distilled methyl iodide, and then the tube was sealed off and shaken at room temperature for 24 h. The contents were fractionally distilled to yield an acetonitrile-water azeotrope (80:20), 1.7 mL, 95% yield.

III. Data and Analysis

Analysis of the hyperfine structure splitting of the $J = 1$ rotational state of $\text{CH}_3^{12}\text{CN}$ and $\text{CH}_3^{13}\text{CN}$ is done in the coupled representation. The analysis in the uncoupled representation is more straightforward but the initial matrices are larger and many more calculations must be performed.

When doing calculations in the coupled scheme, it is very important to define consistent coupling schemes in both the laboratory and molecular frames to obtain a self-consistent set of phase factors for all interactions. In a coupling scheme of the type $J = j_1 + j_2$ it is very important to identify j_1 (and j_2) with the same nucleus for all interactions. The phase factors do not present problems with diagonal matrix elements but can cause errors when more than one term in the Hamiltonian gives off-diagonal matrix elements. The spin-rotation terms are normally defined in the laboratory frame and most easily calculated in that frame. The spin-spin interactions must be calculated in the molecular frame coupling scheme presented by Van Vleck.¹⁷ Attempts to calculate spin-spin interaction matrix elements in the laboratory frame coupling scheme using the methods given by Edmonds¹⁸ will yield incorrect results.

The coupling schemes we used for analysis of $\text{CH}_3^{12}\text{CN}$ and $\text{CH}_3^{13}\text{CN}$ data are as follows.

Table I. Results of Measurements and Calculations for Two-Cavity Measurements on $\text{CH}_3^{12}\text{CN}^a$

F_1'	F'	measd	data	calcd	dev
0	1.5	18 399 891.78	2108.32	2108.29	-0.03
2	2.5	18 398 004.41	220.95	221.04	0.09
2	1.5	18 397 995.60	212.14	{ 213.95 }	-1.26
2	3.5				
2	0.5	18 397 986.77	203.31	203.65	0.34
1	0.5	18 396 734.38	-1049.09	-1049.14	-0.05
1	2.5	18 396 726.02	-1057.45	-1057.37	0.08
1	1.5	18 396 719.79	-1063.68	-1063.74	-0.06

^a The data shown gives measured frequencies relative to the line center at 18 397 783.46 kHz. The standard deviation for the fit is 0.6 kHz. The (F_1', F') = (2, 1.5) and (2, 3.5) components were not resolved.

For the laboratory frame

$$\mathbf{J} + \mathbf{I}_N = \mathbf{F}_1 \quad \mathbf{I}_H + \mathbf{F}_1 = \mathbf{F}_2 \quad \mathbf{I}_C + \mathbf{F}_2 = \mathbf{F}$$

and for the molecular frame

$$\mathbf{J} = \mathbf{F}_1 + \tilde{\mathbf{I}}_N \quad \mathbf{F}_1 = \tilde{\mathbf{I}}_H + \mathbf{F}_2 \quad \mathbf{F}_2 = \mathbf{F} + \tilde{\mathbf{I}}_C$$

where \mathbf{I}_H represents the total spin angular momentum of the protons ($\frac{3}{2}$ here since we observe $K = 0$ states) and \mathbf{I}_C is the spin angular momentum of ^{13}C . The $\tilde{\mathbf{I}}$ are reversed-spin (internal) angular momenta as discussed by Van Vleck.¹⁷ The total laboratory frame angular momentum is denoted by \mathbf{F} and is identical with \mathbf{F}_2 for $\text{CH}_3^{12}\text{CN}$. The terms in the Hamiltonian for the nitrogen quadrupole coupling and nitrogen spin-rotation interactions have been discussed in a number of places^{4,19,20,21} and are not repeated here. The terms in the hyperfine Hamiltonian due to proton and ^{13}C spin-rotation and all spin-spin interactions are as in eq 1, where

$$D_{NN'} = \mu_N \mu_{N'} r_{NN'}^{-3} (3 \cos^2 \beta - 1) / 2$$

$$\Phi(L) = L(L+1)(2L+1)$$

$$\Theta(J) = [1 - \{3K^2/J(J+1)\}][\Phi(J)/(2J-1)(2J+3)]^{1/2}$$

in which β is the angle formed by $r_{NN'}$ and the C_3 axis. These expressions were developed using the methods of Edmonds.¹⁸

The results of the measurements and calculation for $\text{CH}_3^{12}\text{CN}$ are shown in Table I. The coupling parameters obtained here conform to the previous results,⁴ but the confidence in these numbers is increased since all components except one pair of lines was completely resolved. Accurate parameters for $\text{CH}_3^{12}\text{CN}$ were needed to perform the fitting of the $\text{CH}_3^{13}\text{CN}$ data. The $\text{CH}_3^{13}\text{CN}$ data is not so well resolved and can be fit with much more confidence if it is only necessary to adjust the ^{13}C spin-rotation interaction.

The $F_1' = 0$ component of the $J = 1 \rightarrow 0$ transition in $\text{CH}_3^{13}\text{CN}$ is a single line as it is for the ^{12}C molecule, and it was recorded in natural-abundance $\text{CH}_3^{13}\text{CN}$ at 18 390 789.58 kHz as discussed above. The experimental spectrum for this component is shown in Figure 2.

The $F_1' = 1$ and $F_1' = 2$ transitions have six and eight components, respectively, and these were not completely resolved. For these transitions the ^{13}C spin-rotation interaction strength was adjusted to obtain the best fit of the calculated line shapes to the experimental spectra. The ^{13}C -N and ^{13}C -H spin-spin interactions were calculated from the molecular geometry and nuclear magnetic moments.³ The "best-fit" value for the ^{13}C spin-rotation interaction is $C_C = 3.6 \pm 0.2$ kHz. Transition intensities for calculated spectra were computed using relations given by Thaddeus, Krisher, and Loubser.¹⁹ The $F_1' = 2$ components were more sensitive to changes

Table II. Hyperfine Interaction Strengths (kHz) Obtained by Fitting Data for $\text{CH}_3^{12}\text{CN}$ and $\text{CH}_3^{13}\text{CN}$ $J = 1 \rightarrow 0$ Transitions^a

	$\text{CH}_3^{12}\text{CN}$	$\text{CH}_3^{13}\text{CN}$
eqQ	-4224.4 ± 0.7	-4224.6 ± 1.0
C_N	2.0 ± 0.4	1.9 ± 0.5
C_H	-0.6 ± 0.4	
C_C		3.6 ± 0.2
D_{NH}		0.23^b
D_{HH}		20.49^b
D_{HC}		2.06^b
D_{NC}		1.41^b

^a Spin-spin parameters (D_{ij}) were calculated from nuclear moments and molecular geometry. ^b Calculated from nuclear moments and geometry.

$$\begin{aligned} \mathcal{H}' = & C_H (-1)^{J+F_1+F_1'+I_N+I_H+F_2} [\Phi(I_H)\Phi(J)(2F_1+1) \\ & \times (2F_1'+1)]^{1/2} \begin{Bmatrix} F_2 & F_1' & I_H \\ 1 & I_H & F_1 \end{Bmatrix} \begin{Bmatrix} J & F_1' & I_N \\ F_1 & J & 1 \end{Bmatrix} \\ & + C_C (-1)^{I_C+F_2+F_2'+I_H+2F_1+J+I_N} [\Phi(I_C)\Phi(J) \\ & \times (2F_2+1)(2F_2'+1)(2F_1+1)(2F_1'+1)]^{1/2} \\ & \times \begin{Bmatrix} F & F_2' & I_C \\ 1 & I_C & F_2 \end{Bmatrix} \begin{Bmatrix} F_1' & F_2' & I_H \\ F_2 & F_1 & 1 \end{Bmatrix} \begin{Bmatrix} J & F_1' & I_N \\ F_1 & J & 1 \end{Bmatrix} \\ & + D_{NH} \Theta(J) (-1)^{I_H+F_2+F_1} [30\Phi(I_N)\Phi(I_H)(2F_1'+1) \\ & (2F_1+1)]^{1/2} \times \begin{Bmatrix} I_H & F_1' & F_2 \\ F_1 & I_H & 1 \end{Bmatrix} \begin{Bmatrix} F_1' & F_1 & 1 \\ I_N & I_N & 1 \\ J & J & 2 \end{Bmatrix} \\ & + D_{HH} \Theta(J) (-1)^{J+I_N+F_1'+F_1+F_2+3I_H(1/4)} \\ & \times [\Phi(I_H)(2F_1'+1)(2F_1+1)(2I_H-1)(2I_H+3)]^{1/2} \\ & \times \begin{Bmatrix} I_H & F_1' & F_2 \\ F_1 & I_H & 2 \end{Bmatrix} \begin{Bmatrix} F_1' & J & I_N \\ J & F_1 & 2 \end{Bmatrix} \\ & + D_{NC} \Theta(J) (-1)^{F_2+I_H+F_1'+I_C+F_2'+I_C+F} [30\Phi(I_N)\Phi(I_C) \\ & \times (2F_1+1)(2F_1'+1)(2F_2+1)(2F_2'+1)]^{1/2} \\ & \times \begin{Bmatrix} I_C & F_2' & F \\ F_2 & I_C & 1 \end{Bmatrix} \begin{Bmatrix} F_2' & F_1' & I_H \\ F_1 & F_2 & 1 \end{Bmatrix} \begin{Bmatrix} F_1' & F_1 & 1 \\ I_N & I_N & 1 \\ J & J & 2 \end{Bmatrix} \\ & + D_{HC} \Theta(J) (-1)^{F_1+I_N+J+1+I_C+F+F_2} [30\Phi(I_C)\Phi(I_H) \\ & \times (2F_1+1)(2F_1'+1)(2F_2+1)(2F_2'+1)]^{1/2} \\ & \times \begin{Bmatrix} I_C & F_2' & F \\ F_2 & I_C & 1 \end{Bmatrix} \begin{Bmatrix} F_2' & F_2 & 1 \\ I_H & I_H & 1 \\ F_1' & F_1 & 2 \end{Bmatrix} \begin{Bmatrix} F_1' & J & I_N \\ J & F_1 & 2 \end{Bmatrix} \quad (1) \end{aligned}$$

in C_C than the $F_1' = 1$ components. The line-shape-fitting procedure also allowed determinations of center frequencies for $F_1' = 1$ and $F_1' = 2$ groups of components. The parameters obtained are given in Table II.

The experimental and "best-fit" spectra obtained by computer fitting data for $F_1' = 2$ and $F_1' = 1$ groups of lines for $\text{CH}_3^{13}\text{CN}$ are shown in Figure 3. The center frequencies for these groups are 18 388 894.2 kHz for $F_1 = 2$ and 18 387 623.0 kHz for $F_1 = 1$.

IV. ^{13}C Spin Rotation and Magnetic Shielding

The elements of the nuclear magnetic shielding tensor (σ_{xx}) can be written as a sum of the diamagnetic and paramagnetic components.⁵

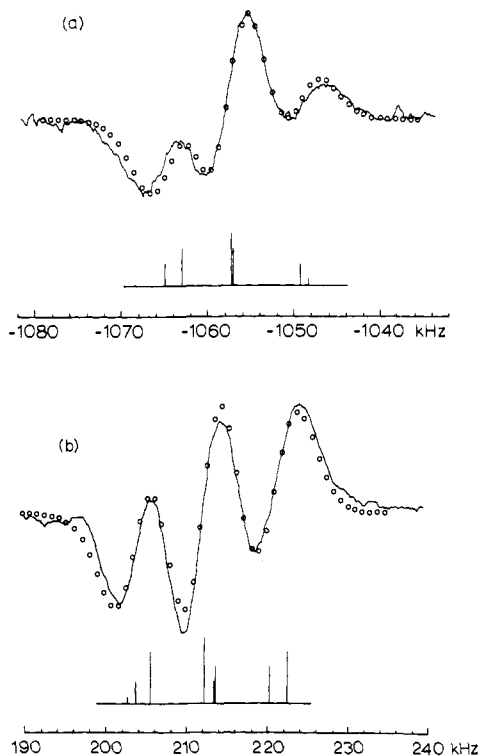


Figure 3. Tracings of experimental spectra and "best-fit" spectra (open circles) obtained by computer fitting for the $F_1 = 1$ (a) and $F_1 = 2$ (b) components of the $J = 1 \rightarrow 0$ transitions in $\text{CH}_3^{13}\text{CN}$. The positions and relative intensities of the components of the two-line groups as obtained by the computer fitting are indicated by the sticks below the spectra. Frequencies are in kilohertz relative to the line center at 18 388 681 kHz.

$$\sigma_{xx} = \sigma_{xx}^d + \sigma_{xx}^p$$

It has recently been shown possible¹⁴ to use semiempirical molecular orbital (MO) theory to obtain diamagnetic shielding components which are in very good agreement with the *ab initio* results and the empirical atom-dipole results.²² Paramagnetic components are much more difficult to calculate by any method, but these may be obtained from the elements of the spin-rotation tensor.^{5,6} There are also two contributions to the elements of the spin-rotation tensor. The classical contribution due to the motion of the molecule may be easily calculated from a knowledge of the molecular geometry, and it is of positive sign. On subtraction of the nuclear contribution from the total measured value, only the electronic part remains. The electronic contributions to the spin-rotation tensor elements are directly proportional to the paramagnetic shielding elements so the paramagnetic term can be written as

$$\sigma_{xx}^p = (M_p/2mg_N)(M_{xx}/G_{xx})$$

$$- (e^2/2mc^2) \sum_n (Z_n/r_n^3)(y_n^2 + z_n^2)$$

where M_p is the proton mass, m is the electronic mass, g_N is the nuclear g value, and M_{xx}/G_{xx} is the ratio of spin-rotation constant to rotational constant in the x direction. The spin-rotation tensor component perpendicular to the symmetry axis (a axis) is

$$C_{\perp} = 3.6 \pm 0.2 \text{ kHz}$$

$$(M_{xx} = -C_{xx}, \text{ so that } M_{\perp} = -3.6 \text{ kHz})$$

From the above equation this leads to a paramagnetic shielding tensor component perpendicular to the symmetry axis:

$$\sigma_{\perp}^p = -418 \pm 14 \text{ ppm}$$

The theoretical value¹⁴ of $\sigma_{\perp}^d = 407 \text{ ppm}$ may be compared with the atom-dipole²⁰ value of 406 ppm.¹² Since *ab initio* values are usually within 1%, we estimate an accuracy of $\pm 4 \text{ ppm}$ for σ_{\perp}^d . Combination of these results

$$\sigma_{\perp} = \sigma_{\perp}^p + \sigma_{\perp}^d = -11 \pm 14 \text{ ppm}$$

corresponds to the gas-phase value of the shielding component perpendicular to the C_3 axis of the $\text{CH}_3^{13}\text{CN}$ molecule. It is of interest to compare this value with those based on recent, direct, condensed-phase NMR measurements. In the cross-polarization experiments on solid $\text{CH}_3^{13}\text{CN}$, Kaplan et al.¹¹ obtained $\sigma_{\parallel} - \sigma_{\perp} = 204 \pm 6 \text{ ppm}$ and an isotropic value of $\bar{\sigma} = 46 \pm 16 \text{ ppm}$ (we are assuming a $\pm 6 \text{ ppm}$ accuracy in the experimental measurement and $\pm 10 \text{ ppm}$ for the absolute scale of ^{13}C chemical shielding¹⁰), and hence for the solid $\sigma_{\perp} = -22 \pm 18 \text{ ppm}$. The two independent NMR studies^{12,13} of $\text{CH}_3^{13}\text{CN}$ oriented in the nematic liquid crystal phase gave results which were within the experimental error. In the first of these¹² $\sigma_{\parallel} - \sigma_{\perp} = 302 \pm 8 \text{ ppm}$, which may be combined with the isotropic liquid value of $76 \pm 10 \text{ ppm}$ to give $\sigma_{\perp} = -25 \pm 13 \text{ ppm}$. Thus, one has the very awkward results that σ_{\perp} for $\text{CH}_3^{13}\text{CN}$ in the condensed phases are within the experimental error of the measurements, despite an approximate 100-ppm disparity in the shielding anisotropy and about a 30-ppm difference in the isotropic shielding values. Our present gas-phase value for σ_{\perp} is in agreement with these values.

An *ab initio* calculation²³ for $\text{CH}_3^{13}\text{CN}$ by means of perturbed Hartree-Fock theory with contracted Gaussian-type orbitals led to values of $\sigma_{\perp} = 10 \text{ ppm}$ and $\sigma_{\parallel} = 290 \text{ ppm}$, so that the calculated anisotropy of 280 ppm is in closer conformity with the liquid-crystal results.

We are not aware of any other study in which gas-phase shielding components have been compared with values obtained in the solid phase. In the multiple-pulse work on solids, it has been consistently noted²⁴ that there is a downfield isotropic shift in going from the liquid to the solid phase. In most cases the shift is not much greater than the experimental errors of 6–14 ppm. However, $\text{CH}_3^{13}\text{CN}$ and C_6F_6 appear to be exceptional with shifts of about 30 and 20 ppm, respectively.

The importance of medium effects and gas-to-solution differences in chemical shifts has been a subject of interest for many years²⁵ and is of particular importance because the calculated results apply to the isolated gas-phase molecule, whereas almost all measurements have been performed in the condensed phases. There have been a number of recent studies²⁶ of the density dependencies of ^{13}C chemical shifts and gas-to-solution values of the isotropic values.

Acknowledgments. Acknowledgment is made to the donors of the Petroleum Research Fund, administered by the American Chemical Society, for partial support of this research. The National Science Foundation, Grant CHE-11860, is also gratefully acknowledged.

References and Notes

- (1) (a) University of Arizona. (b) North Texas State University.
- (2) (a) D. K. Coles, W. E. Good, and R. H. Hughes, *Phys. Rev.*, **79**, 224A (1950); (b) M. Kessler, H. Ring, R. Trambarullo, and W. Gordy, *ibid.*, **79**, 54 (1950).
- (3) C. Costain, *Can. J. Phys.*, **21**, 2431 (1969).
- (4) S. G. Kukolich, D. J. Ruben, J. H. S. Wang, and J. R. Williams, *J. Chem. Phys.*, **58**, 3155 (1973).
- (5) N. F. Ramsey, *Phys. Rev.*, **78**, 699 (1950); N. F. Ramsey, *Molecular Beams*, Oxford University Press, London, 1956, Chapter 6.
- (6) W. H. Flygare, *J. Chem. Phys.*, **41**, 793 (1964); W. Hüttner and W. H. Flygare, *ibid.*, **47**, 4137 (1967).
- (7) S. G. Kukolich, *J. Am. Chem. Soc.*, **97**, 5704 (1975).
- (8) I. Ozier, L. M. Crapo, and N. F. Ramsey, *J. Chem. Phys.*, **49**, 2314 (1968).
- (9) F. H. deLeeuw and A. Dymanus, *Chem. Phys. Lett.*, **7**, 288 (1970).
- (10) B. R. Appleman and B. P. Dailey, *Adv. Magn. Reson.*, **7**, 231 (1974).
- (11) S. Kaplan, A. Pines, R. G. Griffin, and J. S. Waugh, *Chem. Phys. Lett.*, **25**, 78 (1974).
- (12) P. K. Bhattacharyya and B. P. Dailey, *Chem. Phys. Lett.*, **32**, 305 (1975).

- (13) J. D. Kennedy and W. McFarlane, *Mol. Phys.*, **29**, 593 (1975).
(14) M. Barfield and D. M. Grant, *J. Chem. Phys.*, **67**, 3322 (1977). In these results, calculated diamagnetic shielding components agreed with ab initio values to generally better than 1%.
(15) S. G. Kukolich, *Phys. Rev. A*, **138**, 1322 (1965).
(16) J. P. Gordon, *Phys. Rev.*, **99**, 1253 (1955).
(17) J. H. Van Vleck, *Rev. Mod. Phys.*, **23**, 213 (1951).
(18) A. R. Edmonds, "Angular Momentum in Quantum Mechanics", Princeton University Press, Princeton, N.J., 1960.
(19) P. Thaddeus, L. C. Krisher, and J. H. N. Loubser, *J. Chem. Phys.*, **40**, 257 (1964).
(20) P. Thaddeus, L. C. Krisher, and P. Cahill, *J. Chem. Phys.*, **41**, 1542 (1964).
(21) S. G. Kukolich, *Phys. Rev.*, **156**, 83 (1967).
(22) W. H. Flygare and J. Goodisman, *J. Chem. Phys.*, **49**, 3122 (1968); T. D. Gierke, H. L. Tigelaar, and W. H. Flygare, *J. Am. Chem. Soc.*, **94**, 330 (1972); T. D. Gierke and W. H. Flygare, *ibid.*, **94**, 7277 (1972).
(23) R. Ditchfield, D. P. Miller, and J. A. Pople, *J. Chem. Phys.*, **54**, 4186 (1971).
(24) A. Pines, M. G. Gibby, and J. S. Waugh, *J. Chem. Phys.*, **59**, 569 (1973); *Chem. Phys. Lett.*, **15**, 373 (1972).
(25) W. T. Raynes, A. D. Buckingham, and H. J. Bernstein, *J. Chem. Phys.*, **36**, 3481 (1962).
(26) K. Jackowski and W. T. Raynes, *Mol. Phys.*, **34**, 465 (1977); B. Tiffon and J. P. Doucet, *Can. J. Chem.*, **54**, 2045 (1976); D. Cans, B. Tiffon, and J. E. Dubois, *Tetrahedron Lett.*, 2075 (1976).

Calculated ^{13}C NMR Relaxation Parameters for a Restricted Internal Diffusion Model. Application to Methionine Relaxation in Dihydrofolate Reductase

Robert E. London* and John Avitabile

Contribution from Los Alamos Scientific Laboratory, University of California, Los Alamos, New Mexico 87545. Received April 19, 1978

Abstract: ^{13}C NMR relaxation parameters, T_1 , T_2 , and NOE, have been calculated based on a model assuming internal rotational diffusion subject to boundary conditions limiting the range of motion. Numerical results are presented as a function of diffusion coefficients D_0 and D_i and the angle β defined as in the free internal rotation calculation, as well as 2θ , the allowed range of motion. Relaxation times vary from the values expected in the absence of internal motion to values slightly below those calculated using the free internal rotation model as the range is increased from 0 to 360° . The discrepancy in the latter comparison arises from the boundary condition preventing diffusion from 180^+ to 180^- . Changes in T_2 are typically monotonic or nearly monotonic as a function of θ ; however, changes in T_1 and NOE values are markedly nonmonotonic for $D_0 \leq 10^6 \text{ s}^{-1}$ and for certain values of D_i . Criteria for the applicability of the present calculations to the analysis of ^{13}C NMR relaxation data obtained in studies of macromolecules undergoing restricted internal motion have been suggested. The results have been generalized to the case of multiple internal rotations, specifically for the problem of one free and one restricted diffusional process. In general, the two types of rotation are not commutative. This model has been applied to relaxation data recently obtained for the methionine methyl resonances of specifically ^{13}C -labeled dihydrofolate reductase obtained from *S. faecium*. The results indicate that the data can be readily explained by assuming rapid free internal diffusion about the S-CH₃ bond and restricted internal diffusion about the CH₂-S bond of methionine, such that for the broadest resonances the motional range is restricted to $\sim 90^\circ$ and for the sharpest resonances the range is $> 180^\circ$. Restriction of the motion allows a significantly better fit of the data than can be obtained using a model based on two free internal rotations.

I. Introduction

The use of NMR relaxation measurements to obtain dynamic information is based on models which relate the calculated spectral densities to the relevant physical parameters. Models currently in use can be divided into two categories: (1) diffusion over a continuum (isotropic or anisotropic) as described by a diffusion equation¹⁻⁹ or by collision theory¹⁰ and (2) jumps between several discrete states. The second class has been developed extensively to describe the relaxation effects of jumps between discrete states in a variety of solids¹¹ and group-theoretical methods have recently been applied to obtain general solutions.¹² Applications to macromolecules for which overall diffusion is also important have also been developed.^{1,13-17} We have recently shown that a two-state jump model superimposed on overall isotropic diffusion provides a satisfactory approach for the calculation of spin lattice relaxation rates due to ring puckering in proline-containing peptides.¹⁸ Both approaches have been generalized to a series of successive rotations^{14,19} or jumps^{14,17,20} applicable to complex biomolecules. In the present study, a third type of model is considered: free internal diffusion over a restricted range imposed by boundary conditions on the solution of the diffusion equation. Computationally, this approach differs from previous work²¹ in that the relevant autocorrelation

function must be expressed as an infinite series of exponentials. Fortunately, the series is rapidly convergent so that typically only a few terms need be considered. It is thus relatively easy to obtain numerical results for the desired relaxation parameters.

The need for an understanding of the contribution of restricted diffusion to nuclear magnetic relaxation rates arises primarily in the study of complex biomolecules in which restricted internal motion of parts of the molecule is the rule rather than the exception. For example, recent ^{13}C NMR studies of 90% methionine-methyl- ^{13}C labeled dihydrofolate reductase from *S. faecium*²² indicate that internal motion in addition to the expected rapid methyl rotation is significant. Alternatively, the data cannot be explained by using a model which assumes free (unrestricted) rotation about two or more bonds. It was also found that sharper peaks exhibit longer ^{13}C T_1 values and somewhat larger NOE values than broader peaks. However, models based on one or more free internal rotations predict that if the overall motion is in the slow tumbling region, faster internal motion leads to longer T_1 values but smaller NOE values.^{7,23} Thus, explanations of these results using models in which only the rates of internal or overall motion can be varied cannot accommodate the data. The present calculation, while employing idealized boundary conditions, provides a reasonable interpretation of this data